Microchemical Journal 153 (2020) 104454

Contents lists available at ScienceDirect

Microchemical Journal

journal homepage: www.elsevier.com/locate/microc

# Rapid and sensitive detection of synthetic cannabinoids JWH-018, JWH-073 and their metabolites using molecularly imprinted polymer-coated QCM nanosensor in artificial saliva

Semra Akgönüllü[a], Dilek Battal[b,c], M. Serkan Yalcin[d], Handan Yavuz[a], Adil Denizli[a,*]

[a] Department of Chemistry, Faculty of Science, Hacettepe University, Ankara, Turkey
[b] Department of Toxicology, Faculty of Pharmacy, Mersin University, Mersin, Turkey
[c] Department of Toxicology, Faculty of Pharmacy, Near East University, Nicosia, Cyprus
[d] Mersin University, Vocational School of Technical Sciences, Mersin, Turkey

ARTICLE INFO

*Keywords:*
Synthetic cannabinoid
Forensic toxicology
Molecularly imprinted polymers
Nanoparticles
Quartz crystal microbalance
Nanosensor

ABSTRACT

Synthetic cannabinoids (SCs), which are becoming increasingly popular, are an important public health issue considering the common abuse uses and serious adverse effects associated with intoxication. The analysis for controlling the increase in synthetic cannabinoids usage requires a faster and highly sensitive detection that rapidly developing class compounds. In this study, a piezoelectric nanosensor coated with a synthetic biomimetic recognition nanoparticles polymer was designed for the real-time and highly sensitive synthetic cannabinoids (SCs: JWH-018, JWH-073, JWH-018 pentanoic acid and JWH-073 butanoic acid) detection. Synthetic cannabinoids imprinted (MIP) and non-imprinted (NIP) nanoparticles were synthesized. Firstly, the characterization of MIP and NIP nanoparticles were studied by FTIR-ATR, scanning electron microscope, and size measurements. After, nanoparticles were spread onto a quartz crystal microbalance (QCM) chip. Different QCM chip surfaces were studied by contact angle, ellipsometry, and atomic force microscopy measurements. Selective rebinding of target analytes was monitored as a frequency shift measuring mass change with the QCM. Limit of detection values were calculated as 0.28, 0.3, 0.23, 0.29 pg/mL for these SCs in artificial saliva, respectively. The SCs-MIP QCM nanosensors displayed high sensitivity and selectivity in a wide concentration range of SCs (0.0005–1.0 ng/mL) in artificial saliva.

## 1. Introduction

There has been a proliferation at an unprecedented scale of new drug discoveries and syntheses over the last decade, culminating what can be considered to be an issue necessitating global attention and serious public health hazard. Consequently to this rise, a substantial quantity of novel psychoactive substances (NPSs) have become obtainable in illicit drug markets with negligible or non-existent prior knowledge and/or practical experience about their associated health risks, such as side effects or toxicity profiles [1]. Analytical laboratories in the modern age are thus confronted by the challenge of having to account for and adapt to the appearance of such NPSs, which bear the advantage over conventional drugs that they may remain undetected in standard drug testing procedures. Such compounds are also characterized by a scarcity of reliable pharmacological and/or toxicological data, such as their toxicokinetic profiles or detectability in many body matrices. The risks posed do not end with the user either, as many NPSs can also pose risks to non-users, such as in the case of the operation of vehicles or machinery. The operation of vehicles under the influence of drugs (commonly referred to as DUI or DUID) can result in hazardous circumstances and has been indicated as a possible reason for the increase in road accidents [2–4]. Screening tests applied to the detection of NPSs are generally sensitive, inexpensive and rapid but lack high selectivity and thus may be subject to false positives associated with cross-reactivity to similarly-structured by stander drugs [5,6].

Urine is currently the matrix of choice for the evaluation and monitoring of recent drug exposure. It has several advantages, such as an extended envelope of detection, where drug exposure can be detected over the length of several days, and advantages resultant from the characteristics. However, the saliva has been proposed as an alternative matrix that has attracted rising interest in clinical and forensic toxicology, such as workplace drug testing, DUID programs, pain mitigation and management, epidemiological studies [7–12]. Saliva as an analytical matrix bears the advantages of ease of collection, low

* Corresponding author at: Hacettepe University, Department of Chemistry, 06800, Ankara, Turkey.
*E-mail address:* denizli@hacettepe.edu.tr (A. Denizli).

https://doi.org/10.1016/j.microc.2019.104454
Received 1 July 2019; Received in revised form 20 October 2019; Accepted 19 November 2019
Available online 19 November 2019

biohazard risks, and gender neutrality in procurement and monitoring during sample acquisition [13]. Studies conducted on synthetic cannabinoids indicate that only a minor fraction of the parent compound is excreted in unchanged form, where the vast proportion is metabolized into more hydrophilic metabolites [14,15]. Saliva has an additional advantage in that the proportion of parent compounds is more predominant in its matrices, allowing for faster identification of new compounds [16]. Although saliva concentration is not considered to be viable to determine blood concentrations [17–20], the shortness of the detection time in saliva [20], observed after a single intake renders saliva more applicable to identify recent exposure than urine [16]. Saliva can oftentimes be used in DUID determination, workplace drug testing, and monitoring of drug abstinence [21,22]. The primary advantage of saliva in such a testing set is that it allows the setting of the parent compound as a major analytical target. Immunological testing methods utilizing cross-reactions with JWH-018 are already under development for synthetic cannabinoids detection [23,24]. JWH-018 is among the targets of multi-target screening methods employing liquid chromatography–mass spectrometry [25,26]. However, quantitative data are scarce on saliva specimens [23,27,28]. Despite having been isolated first in 2008 [24], JWH-018 was detectable in specimens obtained as late as 2015 [29], therefore it retains its relevance [30]. Among the compounds classified as NPSs, synthetic cannabinoids are considered to hold importance and new members have been continuously introduced [31].

Synthetic cannabinoids (SCs), which mimic the influence of $\Delta^9$-tetrahydrocannabinol ($\Delta^9$-THC), are chemical compounds a major active content of cannabis. In the beginning, they were used as therapeutic agents for pain cure and are linked to cannabinoid receptors in the brain [32]. Unlike the common utilize of marijuana, which poses only relatively limited acute toxicity, serious adverse effects, often requiring medical attention, are not uncommon with SC consumption. Indeed, the relative risk of seeking emergency medical treatment following the use of SCs has been reported to be 30 times higher than that associated with the use of natural forms of cannabis [33]. JWH-018 and JWH-073 are the most well-known aminoalkylindol structure SCs that have appeared as new drugs of abuse being promoted as “legal” marijuana and sold under brand names [32]. The detection of alkyindole derivatives and their metabolites in biological fluids is quite complicated for the low concentration of these compounds [34]. There are several reports about the side effects of SCs including agitation, confusion, dizziness, fast heart beating, and sickness. In human matrices, an assay of SCs is of special importance in areas of clinical and forensic toxicology [35]. Although traditional methods are priceless for conclusive recognition of emerging drugs of abuse, the devices used are naturally expensive and bulky and are not fit for field analysis. There is a requirement for alternative general screening methods that would be sensitive enough for SCs detection in body fluids.

Molecular imprinting technology has been introduced to usher in the in-built designed selectivity towards target analytes by molecularly imprinted polymers (MIPs). MIPs have become very attractive artificial receptor stages for the selective capture of small molecules of structurally similar and related species [36–38]. This mimic recognition based technique, being a type of polymerization, employs the use of the fabrication of specific cavities (binding sites) in a highly polymeric matrix, in such a manner as to be complementary to an analyte designated a target [35,39]. This then permits selective binding between the matrix and the target analyte, even in a chemically complex sample. Due to their high selectivity, MIPs have been used to modify already-existent sensor systems to enhance their performance, such as electrochemical sensors [40,41], optical sensors [42,43], and mass-sensitive sensors [44,45]. Quartz crystal microbalance (QCM) nanosensors are mass-sensitive and have important properties high sensitivity, ease of use, affordability, stability, simplicity and portability. A number of strategies can be developed to design a QCM electrode surface, the most viable approach among these methods is a molecular imprinting strategy [35]. The widespread utilization of molecularly-imprinted polymer coated QCM nanosensors have been published the sensing of various analytes such as proteins [46], enzymes [47], amino acids [48], drugs [49], pesticides [50], metals [51], antibiotics [52], biomarkers [53], bacteria [54,55], pathogens [56], vitamins [57] and low molecular weight molecules [58–61] etc.

The common applications of MIP in the QCM sensor have been reported for different analytes detection but there is no combination of MIP and QCM study to sensing SCs in saliva. Hence, the development of simple monitoring methods for SCs detection in biological materials is required. Herein, we synthesized molecularly-imprinted nanoparticles using mini-emulsion polymerization. Then, the QCM chip surface was coated with SCs-MIP nanoparticles. Detection studies of JWH-018, JWH-073 and their major metabolites were performed using aqueous and artificial saliva solutions. Kinetic results were determined by calculating association kinetics analysis, Scatchard, Langmuir, Freundlich and Langmuir-Freundlich isotherms.

## 2. Experimental

### 2.1. Chemicals

Ethylene glycol dimethacrylate, 2-hydroxyethyl methacrylate, polyvinyl alcohol, ammonium persulfate, sodium dodecyl sulfate, sodium bisulfite and sodium bicarbonate were purchased from Sigma (St. Louis, USA). Naphthalen-1-yl-(1-pentylindol-3-yl)methanone (JWH-018); naphthalen-1-yl-(1-(5-pentanoic acid)-indol-3-yl)-methanone (JWH-018 pentanoic acid); naphthalen-1-yl-(1-butylindol-3-yl)methanone (JWH-073); and naphthalen-1-yl-(1-(4-butanoic acid)-indol-3-yl)-methanone (JWH-073 butanoic acid) were purchased Lipomed (Arlesheim, Switzerland). The other chemicals were supplied from Merck (Darmstadt, Germany). Artificial saliva consisted of the following (deionized water): $CaCl_2{\bullet}2H_2O$, 0.8 mg/mL; KCl, 0.4 mg/mL; NaCl, 0.4 mg/mL; $Na_2S{\bullet}9H_2O$, 0.05 mg/mL; $NaH_2PO_4$, 0.69 mg/mL [62]. The phosphate buffered saline solution (0.1 M PBS, 0.002 M $KH_2PO_4$, 0.137 M NaCl, 0.01 M $Na_2HPO_4$, 0.0027 M KCl, pH 7.4) was used as equilibrium buffer for the QCM nanosensor system.

### 2.2. Synthesis of nanoparticles

Using a two phase mini-emulsion polymerization system were synthesized synthetic cannabinoids imprinted nanoparticles (SCs-MIP). The sodium dodecyl sulfate (14.0 mg), sodium bicarbonate (12.5 mg) and polyvinyl alcohol (93.0 mg) were dissolved in 5.0 mL deionized water as an aqueous phase-I. The sodium dodecyl sulfate (50.0 mg) and polyvinyl alcohol (50.0 mg) was dissolved in 100 mL of deionized water as a phase-II. 1.0 mL ethylene glycol dimethacrylate (EGDMA) and 0.5 mL 2-hydroxyethyl methacrylate (HEMA) was prepared as an organic phase-III. The phase-III was slowly added to phase-I. The mixture was homogenized at 6000 rpm by a homogenizer to obtain a mini-emulsion. After homogenization, synthetic cannabinoid target molecules (0.01 mmol) and N-methacryloyl-(L)-phenylalanine (MAPA) functional monomer (0.01 mmol) were added to the organic phase and mixture was stirred for 2 h to get effectively interactive monomer target pre-polymerization complex. MAPA monomer was utilized as a functional monomer for non-covalent interactions with synthetic cannabinoids and briefly, synthesis procedure and NMR analysis result was given to supplementary material (Fig. S1) [63]. The phase-I and phase-III mixture was added to the phase-II, and the final mixture was stirred in a sealed-cylindrical reactor (Heidolph, Germany) at 500 rpm. In the polymerization temperature (40 °C) solution was easily warmed. After nitrogen gas was flushed through, ammonium persulfate (APS, 50 mg) and sodium bisulfite ($NaHSO_3$, 100 mg) was added to the solution as

initiators. The synthesis conditions were set for 24 h. SCs-MIP NPs were cleaned through centrifugation (Allegra-64R Beckman Coulter, USA) at 40 000 rpm with 50 mL of $H_2O$/EtOH solution (1:1 v/v) for 45 min to remove surfactants, unreacted monomers and initiators for at least 5 times [64]. In the same manner, non-imprinted nanoparticle (NIP) was synthesized without addition of SCs target molecules to polymerization solutions.

### 2.3. Characterization of nanoparticles

Characterization studies of SCs-MIP and NIP nanoparticles were done by using zeta sizer, scanning electron microscope (SEM), and FTIR–ATR. Protocol for nanoparticles size measurement was applied as follows: SCs nanoparticles were dispersed in 3 mL deionized water and placed into a sample holder of the zeta-sizer device (NanoS Malvern Inst., London, UK). The light scattering was performed at an incidence angle of 90° and 25° The number of nanoparticles was analyzed using the light scattering signal. Surface structures of nanoparticles were investigated by scanning electron microscope (Zeiss, Supra55, Germany). Before starting the analysis, the samples were dried. The samples were coated with platinum for providing conductivity. The surface morphology of the nanoparticles was then analyzed at the appropriate magnification and voltage. FTIR-ATR spectra of nanoparticles were recorded by Thermo Fisher Scientific FTIR-ATR spectrophotometry and total light reflection from the surface of nanoparticles was measured at the range 400–4000 $cm^{-1}$.

### 2.4. Preparation of QCM chips

MAXTEK 5 000 000 Hz Cr/Au polished quartz crystal chips were purchased by INFICON from USA. AT-cut quartz (25.4 mm) was selected for its piezoelectric properties and ideal mechanical. QCM chip surface was cleaned by using hot piranha ($H_2SO_4$:$H_2O_2$). Hot piranha solution was spread onto a QCM chip and waited (30 s). After QCM chip was washing with ethanol and dried at 40 °C for 3 h. SCs-MIP nanoparticles (5 μL) were spread onto the electrode surface. QCM chip was dried by using UV light (365 nm, 100 W) for 30 min. SCs-MIP QCM chip was washed with $H_2O$ and ethanol and after dried (Scheme 1).

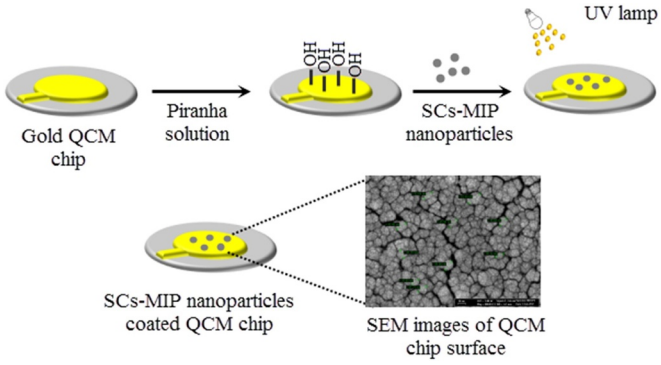


**Scheme 1.** Diagram of molecularly imprinted nanoparticles based QCM chip.

### 2.5. Removal of targets

There are interactions between the MAPA functional monomer and targets resulting from secondary forces. A target molecule can be removed by the breakdown of these interactions. The ethylene glycol/water mixture (50%, v/v) was utilized as a desorption agent. Removal of SCs has performed continuously in the system 30 mL for 2 h. The target molecule was desorbed; the SCs-MIP QCM chips were washed and after dried.

### 2.6. Characterization of SCs-MIP QCM chips

The characterization studies of SCs-MIP and NIP QCM chips were performed using contact angle (CA), ellipsometry, and atomic force microscopy (AFM). The CA of SCs-MIP and NIP QCM chips were analyzed with the sessile drop system by utilization deionized water by KRUSS DSA 100 instrument (Hamburg, Germany). Layer thickness analysis of SCs-MIP and NIP QCM chips were measured using the autonulling ellipsometer (Nanofilm-EP3, Goettingen, Germany). Average layer thickness measurements were done at a wavelength of 532 nm with an incidence angle of 62° AFM (XE-100E, Park System, Korea) analysis of the chip surface was carried out in the non-contact mode. MIP and NIP QCM chips were installed on the device sample holder. 10 μm × 10 μm sample area was displayed with a 256 × 256 pixels resolution. The scan rate was 0.56 Hz. The tests were applied in an air atmosphere.

### 2.7. Monitoring of SCs-MIP QCM nanosensor

SCs-MIP QCM nanosensors were utilized to detection target molecules both an aqueous and artificial saliva samples in real time. Studies were performed with INFICON Maxtek RQCM system (from USA). Sequentially, MIP nanosensors were cleaned by using $H_2O$/MeOH (50%, v/v), pure water and pH 7.4 PBS solution (equilibration buffer). After, the response of SCs-MIP nanosensor was monitored up to stable frequency was observed. Synthetic cannabinoids samples in 0.0005–1.0 ng/mL concentrations range (pH 7.4 PBS 10 mL) were performed to SCs-MIP nanosensor system and frequency shifts were observed (flow rate; 1.0 mL/min). In regeneration step was utilized ethylene glycol/$H_2O$ mixture (20 mL). Then SCs-MIP nanosensors were washed with pure $H_2O$ and pH 7.4 PBS solution was used as equilibration buffer. For each SCs samples applications were repeated with equilibration–adsorption-regeneration steps. The interaction model between target molecules and imprinted QCM nanosensors was determined by using equilibrium kinetic analysis, Scatchard, Langmuir, Freundlich, and Langmuir-Freundlich adsorption isotherm models.

### 2.8. Selectivity, reusability and storage stability

The selectivity of MIPs is principally based on biorecognition [65]. Thus, the selectivity studies of SCs-MIP QCM nanosensors were performed by applying other competitor synthetic cannabinoids in artificial saliva. 1.0 ng/mL of JWH-018, JWH-073 and their metabolites samples were applied to QCM nanosensors system. According to the calculations, the relative selectivity and selectivity coefficients of SCs-MIP and NIP QCM nanosensors were obtained. Reusability studies of SCs-MIP QCM nanosensors were also performed by employing of 0.1 ng/mL JWH-018, 0.01 ng/mL JWH-018 pentanoic acid 0.05 ng/mL JWH-073 and 0.005 ng/mL JWH-073 samples 5 times, consecutively. Stability of SCs-MIP QCM nanosensors was examined by applying the artificial saliva that was prepared in diverse concentrations. Storage stability studies of the SCs-MIP QCM chips were used for 3-repeated, 4 times SCs analysis in 12-month periods and the stability of the QCM chips were observed.

## 3. Results and discussion

### 3.1. Characterization of nanoparticles and QCM chips

A two-phase mini-emulsion polymerization procedure was used to prepare SCs-MIP and NIP nanoparticles. Characterization studies of MIP and NIP nanoparticles were performed using zeta sizer, SEM, and FTIR-ATR spectroscopy. Results obtained from zeta sizer indicated that average particle size MIP and NIP nanoparticles have in the ranges of 38.5 and 45.6 nm with a polydispersity around 0.10–0.16, respectively (Fig. S2, Table S1). Zeta sizer results were confirmed by SEM images of

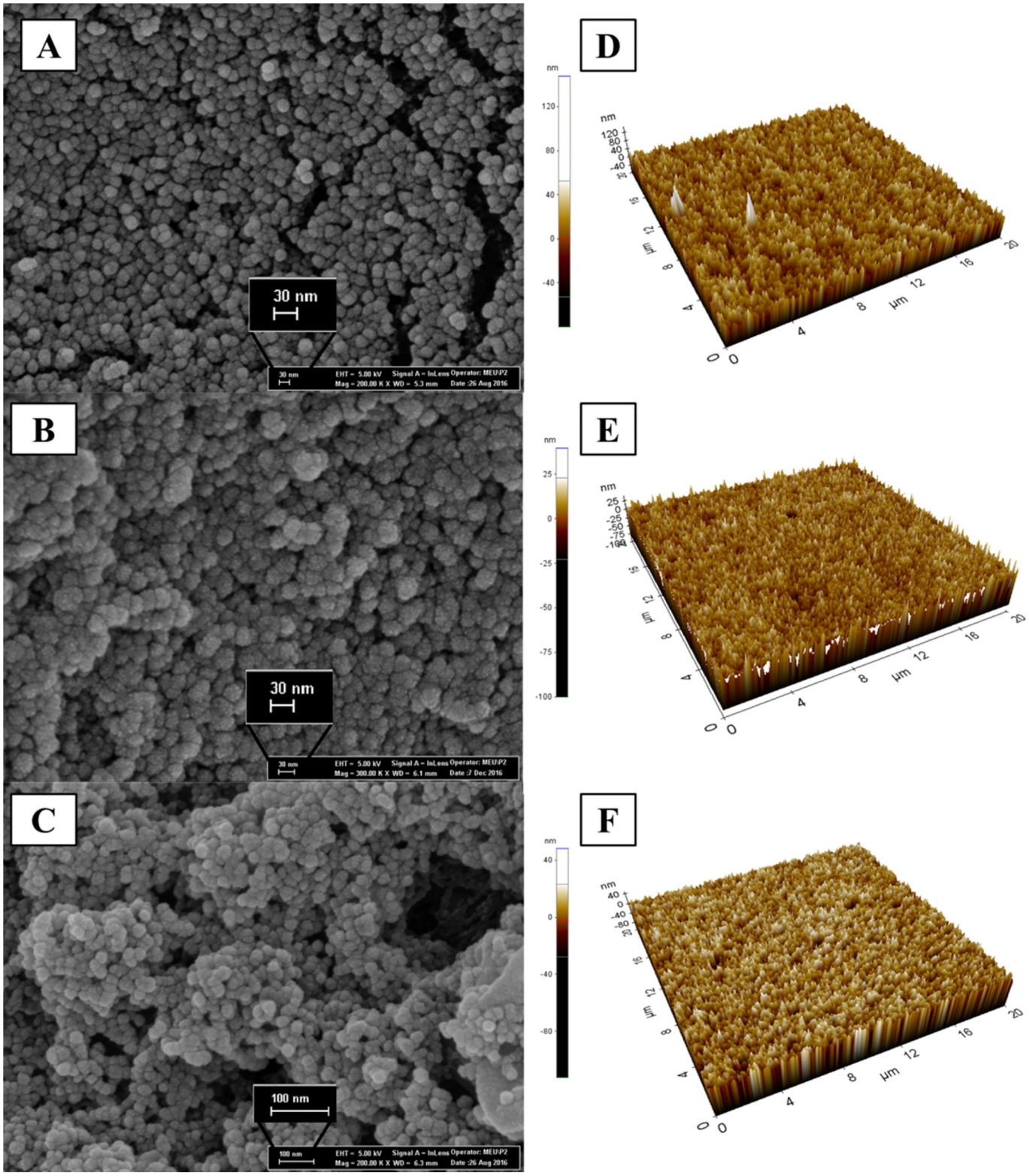


**Fig 1.** SEM image of nanoparticles (A) JWH-073; (B) JWH-018; (C) NIP; and AFM images of SCs-MIP QCM chips (D) JWH-073; (E) JWH-018; (F) NIP.

the nanoparticles. SEM images showed that the MIP and NIP nanoparticles have a mono-size and spherical shape (Fig. 1). In accordance with zeta sizer, SEM results, it can be concluded that the polymerization method was suitable in respect to synthesizing of the mono-sized nanoparticles. This is a significant step which defines adsorption behavior and controls the imprinted cavities homogeneity. FTIR-ATR spectra of the SCs and their metabolite-imprinted nanoparticles and non-imprinted nanoparticles, aliphatic –CH band at 2960 $cm^{-1}$ and carbonyl band at 1720 $cm^{-1}$ were determined. The FTIR spectrum at 1650 and 1550 $cm^{-1}$ attributed to the characteristic amide I and amide II adsorption bands of poly(HEMA–MAPA), respectively. The characteristic frequencies for C—H groups at 1381–1460 $cm^{-1}$ arises from bonding vibration in the poly(HEMA–MAPA) and cannabinoids-imprinted nanoparticles (Fig. S3).

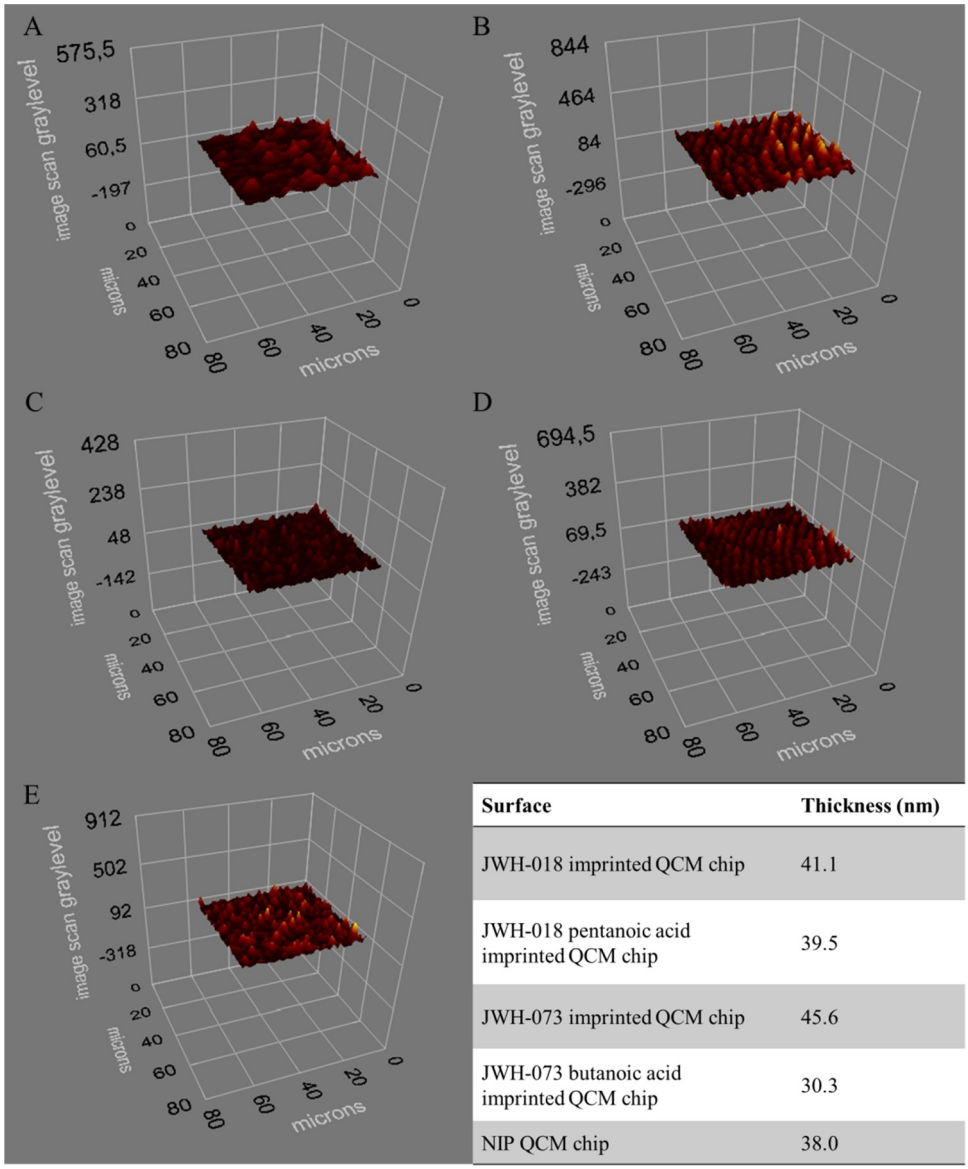


| Surface | Thickness (nm) |
|---|---|
| JWH-018 imprinted QCM chip | 41.1 |
| JWH-018 pentanoic acid imprinted QCM chip | 39.5 |
| JWH-073 imprinted QCM chip | 45.6 |
| JWH-073 butanoic acid imprinted QCM chip | 30.3 |
| NIP QCM chip | 38.0 |

**Fig. 2.** Ellipsometry images of (A) JWH-018; (B) JWH-018 pentanoic acid; (C) JWH-073; (D) JWH-073 butanoic acid-imprinted QCM chips; (E) NIP QCM chip.

Prepared SCs and their major metabolite imprinted, non-imprinted and unmodified QCM chips gold surface were characterized by contact angle (CA), SEM, AFM, and ellipsometry. As presented in Fig. S4, contact angle values of unmodified gold surfaces, NIP, JWH-018, JWH-018 pentanoic acid, JWH-073, and JWH-073 butanoic acid- imprinted QCM chips were obtained as 64.8°, 66.9°, 71.9°, 70.2°, 68.8°, and 67.1°, respectively. The CA values have increased with the imprinting process. This change may be due to the increased hydrophobicity of the surface. AFM analysis of QCM chip surfaces was acquired in non-contact mode (Fig. 1. and Fig S5). The roughness values of NIP, JWH-018, JWH-018 pentanoic acid, JWH-073, and JWH-073 butanoic acid-imprinted chip surfaces are 8.2 nm, 6.8 nm, 9.9 nm, 11.2 nm, and 8.6 nm, respectively. The ellipsometry analysis was carried out and results were presented in Fig. 2. Ellipsometry analysis surface thickness values of JWH-018, JWH-018 pentanoic acid, JWH-073, JWH-073 butanoic acid-imprinted and NIP chip surfaces were found as 41.1 nm, 39.5 nm, 30.3 nm, 45.6 nm, and 38.0 nm, respectively. Thus, we can conclude that the nanoparticles are monolayer and homogeneous. Also, the SEM images of MIP-coated QCM chip surface confirmed the immobilization of the polymer layer and indicated that the homogeneous of the polymer layer (Fig. S6).

### 3.2. QCM nanosensing

#### 3.2.1. Detection of SCs

It is well known that piezoelectric crystals are highly sensitive to pressure and any mass change on their surfaces [35]. The SCs-MIP QCM nanosensor interacted with various concentrations of SCs samples from 0.0005 to 1.0 ng/mL. The Δf and Δm variation graphics against time monitored with SCs-MIP QCM nanosensor utilization of JWH-018, JWH-073 and their metabolites were displayed in Fig S7-8. Δm changes are directly related to increasing concentration of SCs in the sensorgram. As a result, it can be said that SCs-MIP QCM nanosensor has a fast response to synthetic cannabinoids.

The LOD is mostly utilized as evidence of the quality of a sensor. The ability to label-free sensing small amounts of molecules dissolved in a solution using an analytical method or through some type of sensor can be measured by the detection limit. LOD values were calculated using the formula LOD = 3(σ/S) where σ is the standard deviation and S is the sensitivity; the limit of quantification (LOQ 10(σ/S) ≈ 3•LOD) [66–68]. The LOD values were calculated to be 0.28, 0.23, 0.3, 0.29 pg/mL and also LOQ values were calculated to be 3.03, 2.4, 3.0, 3.1 pg/mL of JWH-018, JWH-018 pentanoic acid, JWH-073, and JWH-073

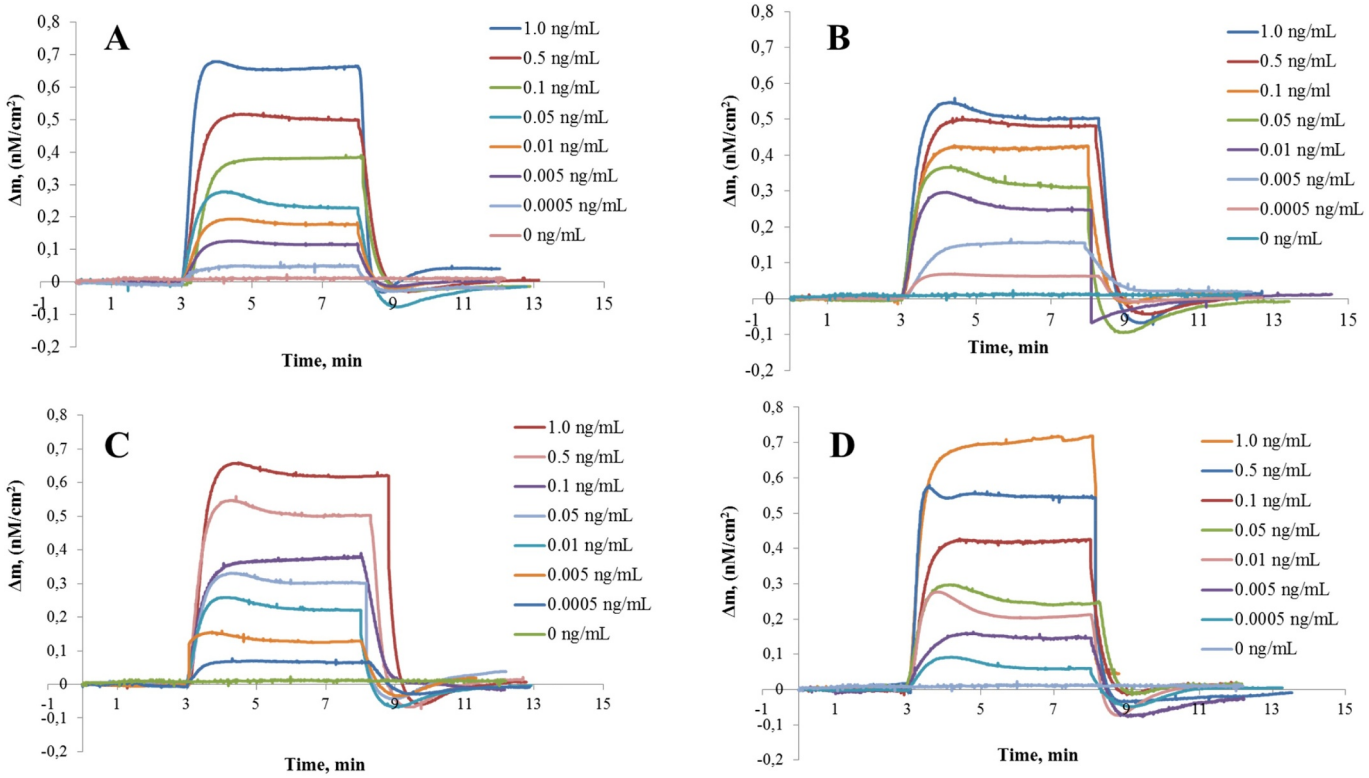


**Fig. 3.** Responses of SCs-MIP QCM nanosensor; (A) JWH-018; (B) JWH-018 pentanoic acid; (C) JWH-073; and (D) JWH-073 butanoic acid.

butanoic acid-imprinted QCM nanosensors. SCs-MIP QCM nanosensors mass shift was shown linearity in a wide range of 0.0005–1.0 ng/mL (Fig S8-11).

Detection of SCs was also performed with SCs-MIP QCM nanosensor in artificial saliva. The artificial saliva was spiked by a different cannabinoid solution concentration of ranging from 0.0005 to 1.0 ng/mL. The changes in SCs-MIP QCM nanosensor mass shift response were performed in proportion to the increase in a spiked synthetic cannabinoids concentration (Fig. 3).

### 3.2.2. Selectivity

The selectivity studies of the each SCs-MIP QCM nanosensors were also carried out for determination of JWH-018, JWH-073, and their metabolites in the artificial saliva. The similar molecular structures of competitor agents were presented (Table 1). 1.0 ng/mL of JWH-018, JWH-073 and their metabolites samples were applied to QCM nanosensors system. For the other SCs samples, each MIP QCM nanosensors displayed the lower response (Fig. 4). The NIP QCM nanosensor mass shifts (Δm) were observed as 0.12, 0.07, 0.09 and 0.04 for JWH-018, JWH-018 pentanoic acid, JWH-073, and JWH-073 butanoic acid, respectively (Fig. 4). Also, responses of NIP QCM nanosensor sensorgram were displayed in Fig. S9. Relative selectivity coefficients (k') determined for every competitor agents were given in Table 2. The relative selectivity coefficient calculated for each target molecule implied that the cavities created in MIP nanoparticles recognized the imprinted template molecule selectively and have a memory of the target molecules.

### 3.2.3. Reusability and storage stability

The reusability is one of the most signification advantages of molecularly imprinted polymer coated QCM nanosensors. The MIP coated QCM chips have a repeatable capacity for reuse because of the stability of the polymeric structure and durability to media conditions. Equilibration–adsorption-regeneration-rebinding cycle was performed subsequently by applying 0.1 ng/mL JWH-018, 0.01 ng/mL JWH-018 pentanoic acid 0.05 ng/mL JWH-073 and 0.005 ng/mL JWH-073 butanoic acid and cannabinoid solutions. Reusability experiments of SCs-MIP QCM nanosensor chips were performed five times and mass shift values were measured. In Fig. 5, the regeneration-rebinding cycles (A) and storage stability (B) for 12 months of SCs-MIP QCM nanosensor were displayed repeated mass shift during the cycles.

### 3.2.4. Recovery

The recovery studies were performed with three different concentrations (0.005, 0.1 and 1.0 ng/mL) of SCs. Table S3 displays the recoveries of SCs in artificial saliva. The recovery values of the designed imprinted QCM nanosensors are between 79.0 and 98.0% with RSD < 5.0. These results show that closeness to %100 results and the values of recovery were all within the acceptable range (Table S3). To evaluate the developed QCM nanosensor method, an Orbitrap-based LC high resolution-MS/MS method was performed also. As a result, the designed SCs-MIP QCM nanosensors have a perfect efficiency in the detection of SCs and their metabolites with the confirmation of a certain Orbitrap-based LC-high resolution-MS/MS method (Supplementary material).

### 3.3. Determination of kinetic constants for SCs detection assay

The interaction model between target molecules and imprinted QCM nanosensors was investigated by carrying out equilibrium kinetic analysis, Scatchard, Langmuir, Freundlich, and Langmuir–Freundlich isotherm models. The applied linear model could be calculated using these equations:

Equilibrium kinetic analysis:

$$d\Delta m/dt = k_a C\Delta m_{max} - (k_a C + k_d)\Delta m \quad (1)$$

Scatchard:

$$\Delta m_{eq}/[C] = K_A(\Delta m_{max} - \Delta m_{eq}) \quad (2)$$

Langmuir:

**Table 1**
Chemical structures and molecular weight of JWH-018, JWH-073, JWH-018 pentanoic acid and JWH-073 butanoic acid.

| | |
|---|---|
| 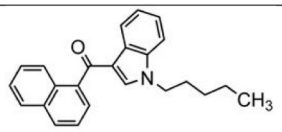 | 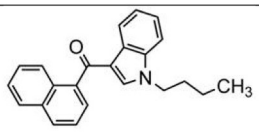 |
| JWH-018 | JWH-073 |
| 341.45 g/mol | 327.42 g/mol |
| 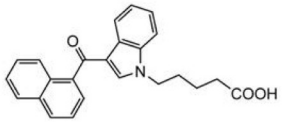 | 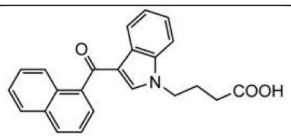 |
| JWH-018 pentanoic acid | JWH-073 butanoic acid |
| 371.43 g/mol | 357.40 g/mol |

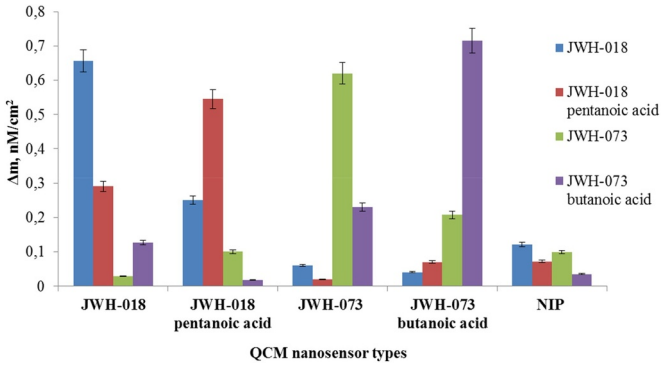


**Fig. 4.** A comparison of the response of SCs-MIP and NIP QCM nanosensor.

$$\Delta m=\{\Delta m_{max}[C]/K_D + [C]\} \quad (3)$$

Freundlich:

$$\Delta m = \Delta m_{max}[C]^{1/n} \quad (4)$$

Langmuir-Freundlich:

$$\Delta m=\{\Delta m_{max}[C]^{1/n}/K_D + [C]^{1/n}\} \quad (5)$$

where Δm is increase in mass (ng/cm$^2$); concentration of SCs: C (ng/mL); forward and reverse kinetic rate: $k_d$ (1/s) and $k_a$ (ng/mL) constants; The $k_a$ and $k_d$ values were calculated by plotting concentrations against the slope of concentrations in the equilibrium kinetic analysis. Freundlich exponent: 1/n; dissociation and association equilibrium: $K_D$ (mL/ng) and $K_A$ (ng/mL) constants; subscripts: maximum (max) and equilibrium (eq) [66]. Langmuir's theory concerns to a uniform surface with equivalent adsorption sites (homogeneous adsorption), which each analyte has constant enthalpies and adsorption activation energy (all sites have the same affinity), with no transmigration of the polymer surface [69,70]. Adsorption isotherm models were applied to identify the homogeneity of SCs-MIP nanoparticles (Table S2). All isotherms, except Langmuir, have high correlation coefficients ($R^2 > 0.94$). The linear fit with the Langmuir equation was comparably the best, which means that the binding of SCs molecules onto SCS imprinted QCM nanosensor is monolayer. Also, Scatchard curve shows some surface homogeneity. Compatibility of $\Delta m_{max}$ values with experimental $\Delta m_{max}$ value shows that the binding of SCs onto SCs-MIP QCM nanosensor polymer surface is homogeneous (Fig. S10-13). The determined parameters for all adsorption models are shown in Table S3.

**Table 2**
SCs-MIP QCM nanosensor the selectivity coefficients (k) and relative selectivity coefficients (k') values.

| MIP SCs | Δm | k | NIP Δm | k | k' | MIP SCs | Δm | k | NIP Δm | k | k' |
|---|---|---|---|---|---|---|---|---|---|---|---|
| **JWH-018** | 0.65 | – | 0.12 | – | – | **JWH-018 pentanoic acid** | 0.55 | – | 0.07 | – | – |
| **JWH-018 pentanoic acid** | 0.29 | 2.24 | 0.07 | 1.71 | 1.31 | **JWH-018** | 0.25 | 2.20 | 0.12 | 0.58 | 3.77 |
| **JWH-073** | 0.03 | 21.67 | 0.09 | 1.33 | 16.25 | **JWH-073** | 0.10 | 5.50 | 0.09 | 0.78 | 7.07 |
| **JWH-073 butanoic acid** | 0.13 | 5.00 | 0.04 | 3.00 | 1.67 | **JWH-073 butanoic acid** | 0.02 | 27.50 | 0.04 | 1.75 | 15.71 |

| MIP SCs | Δm | k | NIP Δm | k | k' | MIP SCs | Δm | k | NIP Δm | k | k' |
|---|---|---|---|---|---|---|---|---|---|---|---|
| **JWH-073** | 0.62 | – | 0.09 | – | – | **JWH-073 butanoic acid** | 0.72 | – | 0.04 | – | – |
| **JWH-073 butanoic acid** | 0.23 | 2.70 | 0.04 | 2.25 | 1.20 | **JWH-073** | 0.21 | 3.43 | 0.09 | 0.44 | 7.71 |
| **JWH-018** | 0.06 | 10.33 | 0.12 | 0.75 | 13.78 | **JWH-018** | 0.04 | 18.00 | 0.12 | 0.33 | 54.00 |
| **JWH-018 pentanoic acid** | 0.02 | 31.00 | 0.07 | 1.29 | 24.11 | **JWH-018 pentanoic acid** | 0.07 | 10.28 | 0.07 | 0.57 | 18.00 |

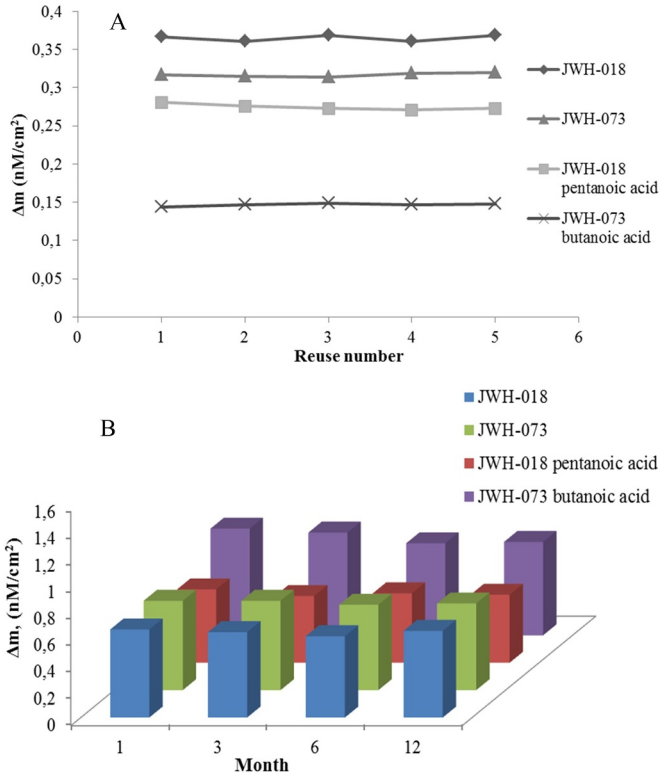


**Fig. 5.** SCs-MIP QCM nanosensor response; (A) Reusability and (B) Storage stability.

## 4. Conclusions

The toxicity of the SCs appears to be worse than that of natural cannabis likely due to the higher potency. In certain circumstances, acute toxic effects can contribute to death. For this reason, in clinical and forensic settings it is fundamental to supply methods targeting these compounds and their major metabolites in saliva samples as well. In this research, QCM nanosensors coated with synthetic biomimetic recognition nanoparticles have been designed for real-time and highly sensitive synthetic cannabinoids (JWH-018, JWH-073 and their major metabolites) detection in artificial saliva. LOD values were calculated to be 0.28, 0.23, 0.3, 0.29 pg/mL JWH-018, JWH-018 pentanoic acid, JWH-073, and JWH-073 butanoic acid in artificial saliva, respectively. In this research, label-free and rapid QCM nanosensor were designed and displayed that the highly selective and sensitive of these QCM nanosensors on aqueous solutions and oral fluid (artificial saliva) at 0.0005–1.0 ng/mL concentrations. QCM is a powerful device in monitoring specific interactions. Although the research we conducted in this critical area needs to be done in different mediums and different SCs types, we confidence that presented strategy represents a pathway for the designer of MIP-based nanosensor indicating a way to form a MIP NPs coated surface directly on the sensor transducer surface which makes it possible to obtain appropriate real-time and label-free of a target molecules.

## Acknowledgements

This study was supported by The Scientific and Technological Research Council of Turkey (TUBITAK); (Project grant no: 215S945).

## Supplementary materials

Supplementary material associated with this article can be found, in the online version, at doi:10.1016/j.microc.2019.104454.

## References

[1] O. Corazza, A Roman-Urrestarazu, Novel Psychoactive Substances Policy, Economics and Drug Regulation, Springer Nature, Switzerland, 2017https://doi.org/10.1007/978-3-319-60600-2.
[2] M. Concheiro, A. deCastro, O. Quintela, M.L. Rivadulla, A. Cruz, Determination of drugs of abuse and their metabolites in human plasma by liquid chromatography–mass spectrometry: an application to 156 road fatalities, J. Chromatogr. B. 17 (2006) 81–89 https://doi.org/10.1016/j.jchromb.2005.12.047.
[3] S. Napoletano, C. Montesano, D. Compagnone, R. Curini, G. D'ascenzo, C. Roccia, M. Sergi, Determination of illicit drugs in urine and plasma by micro-spe followed by HPLC–MS/MS, Chromatographia 75 (2012) 55–63 https://doi.org/10.1007/s10337-011-2156-6.
[4] A.G. Verstraete, Oral fluid testing for driving under the influence of drugs: history, recent progress and remaining challenges, Forensic Sci. Int. 150 (2005) 143–150, https://doi.org/10.1016/j.forsciint.2004.11.023.
[5] P. Amaratunga, B.L. Lemberg, D. Lemberg, Quantitative measurement of synthetic cathinones in oral fluid, J. Anal. Toxicol. 37 (2013) 622–628 https://doi.org/10.1093/jat/bkt080.
[6] R. Rocchi, M.C. Simeoni, C. Montesano, G. Vannutelli, R. Curini, M. Sergi, D. Compagnone, Analysis of new psychoactive substances in oral fluids by means of microextraction by packed sorbent followed by ultra-high performance liquid chromatography–tandem mass spectrometry, Drug Test Anal. 10 (2018) 865–873 https://doi.org/10.1002/dta.2330.
[7] M. Jarvis, J. Williams, M. Hurford, D. Lindsay, P. Lincoln, L. Giles, P. Luongo, T. Safarian, Appropriate use of drug testing in clinical addiction medicine, J. Addict. Med. 11 (3) (2017) 163–173 https://doi.org/10.1097/ADM.0000000000000323.
[8] L. Degenhardt, W. Hall, Extent of illicit drug use and dependence, and their contribution to the global burden of disease, Lancet 379 (9810) (2012) 55–70 https://doi.org/10.1016/S0140-6736(11)61138-0.
[9] H. Reddon, M.J. Milloy, A. Simo, J. Montaner, E. Wood, T. Kerr, Methadone maintenance therapy decreases the rate of antiretroviral therapy discontinuation among HIV-positive illicit drug users, AIDS Behav. 18 (4) (2014) 740–746, https://doi.org/10.1007/s10461-013-0584-z.
[10] F.L. Altice, A. Kamarulzaman, V.V. Soriano, M. Schechter, G.H. Friedland, Treatment of medical, psychiatric, and substance-use comorbidities in people infected with HIV who use drugs, Lancet 376 (9738) (2010) 367–387 https://doi.org/10.1016/S0140-6736(10)60829-X.
[11] C.H. Hinkin, T.R. Barclay, S.A. Castellon, A.J. Levine, R.S. Durvasula, S.D. Marion, H.F. Myers, D. Longshore, Drug use and medication adherence among HIV-1 infected individuals, AIDS Behav. 11 (2) (2007) 185–194, https://doi.org/10.1007/s10461-006-9152-0.
[12] W.M. Bosker, M.A. Huestis, Oral fluid testing for drugs of abuse, Clin. Chem. 55 (11) (2009) 1910–1931, https://doi.org/10.1373/clinchem.2008.108670.
[13] V. Blandino, J. Wetzel, J. Kim, P. Haxhi, R. Curtis, M. Concheiro, Oral fluid vs. urine analysis to monitor synthetic cannabinoids and classic drugs recent exposure, Curr. Pharm. Biotechnol. 18 (10) (2017) 796–805 https://doi.org/10.2174/1389201018666171122113934.
[14] T. Sobolevsky, I. Prasolov, G. Rodchenkov, Detection of JWH-018 metabolites in smoking mixture postadministration urine, Forensic Sci. Int. 200 (1–3) (2010) 141–147, https://doi.org/10.1016/j.forsciint.2010.04.003.
[15] C.L. Moran, V.H. Le, K.C. Chimalakonda, et al., Quantitative measurement of JWH-018 and JWH-073 metabolites excreted in human urine, Anal. Chem. 83 (11) (2011) 4228–4236 https://doi.org/10.1021/ac2005636.
[16] E.L. Øiestad, Å. Øiestad, A. Gjelstad, R. Karinen, Oral fluid drug analysis in the age of new psychoactive substances, Bioanalysis 8 (7) (2016) 691–710 https://doi.org/10.4155/bio-2015-0027.
[17] S.M.R. Wille, E. Raes, P. Lillsunde, T. Gunnar, M. Laloup, N. Samyn, A.S. Christophersen, M.R. Moeller, K.P. Hammer, A.G. Verstraete, Relationship between oral fluid and blood concentrations of drugs of abuse in drivers suspected of driving under the influence of drugs, Ther. Drug Monit. 31 (4) (2009) 511–519 https://doi.org/10.1097/FTD.0b013e3181ae46ea.
[18] K. Langel, H. Gjerde, D. Favretto, P. Lillsunde, E.L. Øiestad, S.D. Ferrara, A.G. Verstraete, Comparison of drug concentrations between whole blood and oral fluid, Drug Test. Anal. 6 (5) (2014) 461–471 https://doi.org/10.1002/dta.1532.
[19] H. Gjerde, K. Langel, D. Favretto, A.G. Verstraete, Detection of illicit drugs in oral fluid from drivers as biomarker for drugs in blood, Forensic Sci. Int 256 (2015) 42–45 https://doi.org/10.1016/j.forsciint.2015.06.027.
[20] A.G. Verstraete, Detection times of drugs of abuse in blood, urine, and oral fluid, Ther. Drug Monit. 26 (2) (2004) 200–205 PMID:15228165.
[21] J.N. Scherer, T.R. Fiorentin, B.T. Borille, G. Pasa, T.R.V. Sousa, L. von Diemen, R.P. Limberger, F. Pechansky, Reliability of point-of-collection testing devices for drugs of abuse in oral fluid: a systematic review and meta-analysis, J. Pharm. Biomed. Anal. 143 (2017) 77–85 https://doi.org/10.1016/j.jpba.2017.05.021.
[22] W.M. Bosker, M.A. Huestis, Oral fluid testing for drugs of abuse, Clin. Chem. 55 (11) (2009) 1910–1931 https://doi.org/0.1373/clinchem.2008.108670.
[23] W.C. Rodrigues, P. Catbagan, S. Rana, G. Wang, C. Moore, Detection of synthetic cannabinoids in oral fluid using ELISA and LC-MS-MS, J Anal. Toxicol. 37 (8) (2013) 526–533 https://doi.org/10.1093/jat/bkt067.
[24] E.L. Øiestad, Å. Øiestad, A. Gjelstad, R. Karinen, Oral fluid drug analysis in the age of new psychoactive substances, Bioanalysis 8 (7) (2016) 691–710 https://doi.org/10.4155/bio-2015-0027.
[25] A. de Castro, B. Piñeiro, E. Lendoiro, A. Cruz, M. López-Rivadulla, Quantification of selected synthetic cannabinoids and Δ9-tetrahydrocannabinol in oral fluid by liquid chromatography–tandem mass spectrometry, J. Chromatogr. A. 1295 (2013)

99–106 https://doi.org/10.1016/j.chroma.2013.04.035.
[26] E.L. Oiestad, U. Johansen, A.S. Christophersen, R. Karinen, Screening of synthetic cannabinoids in preserved oral fluid by UPLC-MS/MS, Bioanalysis 5 (18) (2013) 2257–2268 https://doi.org/10.4155/bio.13.182.
[27] C. Coulter, M. Garnier, C. Moore, Synthetic cannabinoids in oral fluid, J. Anal. Toxicol. 35 (7) (2011) 424–430 PMID:21871150.
[28] S. Kneisel, V. Auwärter, J. Kempf, Analysis of 30 synthetic cannabinoids in oral fluid using liquid chromatography-electrospray ionization tandem mass spectrometry, Drug Test Anal. 5 (8) (2013) 657–669 https://doi.org/10.1002/dta.1429.
[29] F. Franz, V. Angerer, H. Jechle, M. Pegoro, H. Ertl, G. Weinfurtner, D. Janele, C. Schlögl, M. Friedl, S. Gerl, R. Mielke, R. Zehnle, M. Wagner, B. Moosmann, V. Auwärter, Immunoassay screening in urine for synthetic cannabinoids -an evaluation of the diagnostic efficiency, Clin. Chem. Lab. Med. 55 (9) (2017) 1375–1384 https://doi.org/10.1515/cclm-2016-0831.
[30] S.W. Toennes, A. Geraths, W. Pogoda, A. Paulke, C. Wunder, E.L. Theunissen, J.G. Ramaekers, Pharmacokinetic properties of the synthetic cannabinoid JWH-018 in oral fluid after inhalation, Drug Test Anal. 10 (2018) 644–650 https://doi.org/10.1002/dta.2310.
[31] P.O.M. Gundersen, O. Spigset, M. Josefsson, Screening, quantification, and confirmation of synthetic cannabinoid metabolites in urine by UHPLC–QTOF–MS, Drug Test Anal. 11 (2019) 51–67 https://doi.org/10.1002/dta.2464.
[32] S. Tai, W.E. Fantegrossi, Pharmacological and toxicological effects of synthetic cannabinoids and their metabolites, Curr. Top. Behav. Neurosci. 32 (2017) 249–262, https://doi.org/10.1007/7854_2016_60.
[33] C. Deriu, I. Conticello, A.M. Mebel, B. McCord, Micro solid phase extraction surface-enhanced raman spectroscopy (μ-SPE/SERS) screening test for the detection of the synthetic cannabinoid JWH-018 in oral fluid, Anal. Chem. 91 (7) (2019) 4780–4789, https://doi.org/10.1021/acs.analchem.9b00335.
[34] A. Cannaert, J. Storme, F. Franz, V. Auwärter, C.P. Stove, Detection and activity profiling of synthetic cannabinoids and their metabolites with a newly developed bioassay, Anal. Chem. 88 (2016) 11476–11485, https://doi.org/10.1021/acs.analchem.6b02600.
[35] D. Battal, S. Akgönüllü, M.S. Yalcin, H. Yavuz, A. Denizli, Molecularly imprinted polymer based quartz crystal microbalance sensor system for sensitive and label-free detection of synthetic cannabinoids in urine, Biosens. Bioelectron. 111 (2018) 10–17, https://doi.org/10.1016/j.bios.2018.03.055.
[36] X.-T. Ma, X.-W. He, W.-Y. Li, Y.-K. Zhang, Oriented surface epitope imprinted polymer-based quartz crystal microbalance sensor for cytochrome c, Talanta 191 (2019) 222–228, https://doi.org/10.1016/j.talanta.2018.08.079.
[37] V. Safran, I. Göktürk, A. Derazshamshir, F. Yılmaz, N. Sağlam, A. Denizli, Rapid sensing of $Cu^{+2}$ in water and biological samples by sensitive molecularly imprinted based plasmonic biosensor, Microchem. J. 148 (2019) 141–150 https://doi.org/10.1016/j.microc.2019.04.069.
[38] S. Wagner, J. Bell, M. Biyikal, K. Gawlitza, K. Rurack, Integrating fluorescent molecularly imprinted polymer (MIP) sensor particles with a modular microfluidic platform for nanomolar small-molecule detection directly in aqueous samples, Biosens. Bioelectron. 99 (2018) 244–250 https://doi.org/10.1016/j.bios.2017.07.053.
[39] Y. Saylan, S. Akgönüllü, H. Yavuz, S. Ünal, A. Denizli, Molecularly imprinted polymer based sensors for medical applications, Sensors 19 (2019) 1279 https://doi.org/10.3390/s19061279.
[40] B. Song, Y. Zhou, H. Jin, T. Jing, T. Zhou, Q. Hao, Y. Zhou, S. Mei, Y. Lee, Selective and sensitive determination of erythromycin in honey and dairy products by molecularly imprinted polymers based electrochemical sensor, Microchem. J. 116 (2014) 183–190 https://doi.org/10.1016/j.microc.2014.05.010.
[41] R. Gui, H. Jin, H. Guo, Z. Wang, Recent advances and future prospects in molecularly imprinted polymers-based electrochemical biosensors, Biosens. Bioelectron. 100 (2018) 56–70 https://doi.org/10.1016/j.bios.2017.08.058.
[42] Y. Saylan, S. Akgönüllü, D. Cimen, N. Bereli, F. Yılmaz, A. Denizli, Development of surface plasmon resonance sensors based on molecularly imprinted nanofilms for sensitive and selective detection of pesticides, Sens. Actuator B 241 (2017) 446–454 https://doi.org/10.3390/s19061279.
[43] M. Koca Esentürk, S. Akgönüllü, F. Yılmaz, A. Denizli, Molecularly imprinted based surface plasmon resonance nanosensors for microalbumin detection, J. Biomater. Sci. Polym. Ed. 30 (8) (2019) 646–661 https://doi.org/10.1080/09205063.2019.1600181.
[44] Min-Jin Hwang, Wang-Geun Shim, Soon-Do Yoon, Hee Moon, Adsorption of toxic gases on molecularly imprinted polymer coated QCM: measurements and modeling for partial pressure in gas mixture, Adsorption (2019), https://doi.org/10.1007/s10450-019-00074-w.
[45] X. Qiu, X.Y. Xu, X. Chen, Y. Wu, H. Guo, Preparation of a molecularly imprinted sensor based on quartz crystal microbalance for specific recognition of sialic acid in human urine, Anal. Bioanal. Chem. 410 (2018) 4387–4395 https://doi.org/10.1007/s00216-018-1094-7.
[46] M. Bakhshpour, E. Özgür, N. Bereli, A. Denizli, Microcontact imprinted quartz crystal microbalance nanosensor for protein C recognition, Colloid. Surface B 151 (2017) 264–270, https://doi.org/10.1016/j.colsurfb.2016.12.022.
[47] N.A. Karaseva, B. Pluhar, E.A. Beliaev, T.N. Ermolaev, B. Mizaikoff, Synthesis and application of molecularly imprinted polymers for trypsin piezoelectric sensors, Sens. Actuator B 280 (2019) 272–279 https://doi.org/10.1007/s00216-012-6639-6.
[48] F. Liu, X. Liu, S.C. Ng, H. Sze-On Chan, Enantioselective molecular imprinting polymer coated QCM for the recognition of L-tryptophan, Sens. Actuator B 113 (2006) 234–240 https://doi.org.10.1016/j.snb.2005.02.058.
[49] M. Eslami, N. Alizadeh, Nanostructured conducting molecularly imprinted polypyrrole based quartz crystal microbalance sensor for naproxen determination and its electrochemical impedance study, RSC Adv. 6 (2016) 9387–9395 https://doi.org/10.1039/C5RA21489K.
[50] N. Gao, J. Dong, M. Liu, B. Ning, C. Cheng, C. Guo, C. Zhou, Y. Peng, J. Bai, Z. Gao, Development of molecularly imprinted polymer films used for detection of profenofos based on a quartz crystal microbalance sensor, Analyst 137 (2012) 1252–1258 https://doi.org/10.1039/C2AN16120F.
[51] P.G. Su, F.C. Hung, P.H. Lin, Fabrication, characterization and sensing properties of Cu(II) ion imprinted sol–gel thin film on QCM, Mater. Chem. Phys. 135 (2012) 130–136 https://doi.org/10.1016/j.matchemphys.2012.04.035.
[52] M. Pan, Y. Gu, M. Zhang, J. Wang, Y. Yun, S. Wang, Reproducible molecularly imprinted QCM sensor for accurate, stable, and sensitive detection of enrofloxacin residue in animal-derived foods, food analytical methods, Food Anal. Methods 11 (2018) 495–503 https://doi.org/10.1007/s12161-017-1020-1.
[53] X. Qiu, X.-Y. Xu, X. Chen, Y. Wu, H. Guo, Preparation of a molecularly imprinted sensor based on quartz crystal microbalance for specific recognition of sialic acid in human urine, Anal. Bioanal. Chem. 410 (2018) 4387–4395 https://doi.org/10.1007/s00216-018-1094-7.
[54] N. Gupta, R.S. Singh, K. Shah, R. Prasad, M. Singh, Epitope imprinting of iron binding protein of Neisseria meningitidis bacteria through multiple monomers imprinting approach, J. Mol. Recognit. 18 (2018) 2709 https://doi.org/10.1002/jmr.2709.
[55] R. Samardzic, H.F. Sussitz, N. Jongkon, P.A. Lieberzeit, Quartz crystal microbalance in-line sensing of *escherichia coli* in a bioreactor using molecularly imprinted polymers, Sens. Lett. 12 (2014) 1152–1155 https://doi.org/10.1166/sl.2014.3201.
[56] H.Gong B.Yang, C. Chen, X. Chen, C. Cai, A virus resonance light scattering sensor based on mussel-inspired molecularly imprinted polymers for high sensitive and high selective detection of hepatitis a virus, Biosens. Bioelectron. 87 (2017) 679–685, https://doi.org/10.1016/j.bios.2016.08.087.
[57] L. Elmlund, S. Suriyanarayanan, J.G. Wiklander, T. Aastrup, I.A. Nicholls, Biotin selective polymer nano-films, J. Nanobiotechnol. 12 (2014) 8 https://doi.org/10.1186/1477-3155-12-8.
[58] M. Ávila, M. Zougagh, A. Escarpa, Á. Ríos, Supported liquid membrane-modified piezoelectric flow sensor with molecularly imprinted polymer for the determination of vanillin in food samples, Talanta 72 (4) (2007) 1362–1369 https://doi.org/10.1016/j.talanta.2007.01.045.
[59] J. Alenus, A. Ethirajan, F. Horemans, A. Weustenraed, P. Csipai, J. Gruber, M. Peeters, T.J. Cleij, P. Wagner, Molecularly imprinted polymers as synthetic receptors for the QCM-D-based detection of L-nicotine in diluted saliva and urine samples, Anal. Bioanal. Chem. 405 (2013) 6479–6487 https://doi.org/10.1007/s00216-013-7080-1.
[60] Y. Fu, H.O. Finklea, Quartz crystal microbalance sensor for organic vapor detection based on molecularly imprinted polymers, Anal. Chem. 75 (20) (2003) 5387–5393 https://doi.org/10.1021/ac034523.
[61] J. Dai, Y. Zhang, M. Pan, L. Kong, S. Wang, Development and application of quartz crystal microbalance sensor based on novel molecularly imprinted sol–gel polymer for rapid detection of histamine in foods, J. Agric. Food Chem. 62 (23) (2014) 5269–5274 https://doi.org/10.1021/jf501092u.
[62] G. Yıldırmaz, S. Akgöl, M.Y. Arıca, H. Sönmez, A. Denizli, Polyhydroxyethyl methacrylate/polyhydroxybutyrate composite membranes for fluoride release, J. Appl. Poly. Sci. 87 (2003) 976–981 https://doi.org/10.1002/app.11397.
[63] S. Akgönüllü, H. Yavuz, A. Denizli, Preparation of imprinted cryogel cartridge for chiral separation of L-phenylalanine, Artif. Cell Nanomed. B. 45 (4) (2016) 800–807 https://doi.org/10.1080/21691401.2016.1175445.
[64] B. Lin, L. Wan, X. Sun, C. Huang, S. Pedersen-Bjergaard, X. Shen, Electromembrane extraction of high level substances: a novel approach for selective recovery of templates in molecular imprinting, J. Membrane Sci 568 (2018) 30–39 https://doi.org/10.1016/j.memsci.2018.09.056.
[65] Jianming Pan, Wei Chen, Yue Ma, Guoqing Pan, Molecularly imprinted polymers as receptor mimics for selective cell recognition, Chem. Soc. Rev. 47 (2018) 5574–5587 https://doi.org/10.1039/C7CS00854F.
[66] S. Koyun, S. Akgönüllü, H. Yavuz, A. Erdem, A. Denizli, Surface plasmon resonance aptasensor for detection of human activated protein C, Talanta 194 (2019) 528–533 https://doi.org/10.1016/j.talanta.2018.10.007.
[67] Á. Lavín, J. de Vicente, M. Holgado, M.F. Laguna, R. Casquel, B. Santamaría, M.V. Maigler, A.L. Hernández, Y. Ramírez, On the determination of uncertainty and limit of detection in label-free biosensors, Sensors 18 (2018) 38 https://doi.org/10.3390/s18072038.
[68] D. Desai, A. Kumar, D. Bose, M. Datta, Ultrasensitive sensor for detection of early stage chronic kidney disease in human, Biosens. Bioelectron. 105 (2018) 90–94 https://doi.org/10.1016/j.bios.2018.01.031.
[69] S. Gomri, J.-L. Seguin, J. Guerin, K. Aguir, Adsorption–desorption noise in gas sensors: modelling using Langmuir and Wolkenstein models for adsorption, Sens. Actuator B 114 (1) (2006) 451–459 https://doi.org/10.1016/j.snb.2005.05.033.
[70] K.Y. Foo, B.H. Hameed, Insights into the modeling of adsorption isotherm systems, Chem. Eng. J. 156 (1) (2010) 2–10 https://doi.org/10.1016/j.cej.2009.09.013.